Supplementary Material to the article

"Photonic spin Hall effect in subwavelength diffraction gratings"

The electric field of the reflected beam can be described using the standard SHEL (spin Hall effect of light) theory [1-3]. The complex amplitude of the reflected beam can be expressed as Fourier transformation:

$$\mathbf{E}(x_r, y_r, z_r) = \iint \mathbf{E}\left(k_{rx}, k_{ry}, z_r\right) e^{ik_{rx}x + ik_{ry}y} dk_{rx} dk_{ry}, \tag{S1}$$

where the angular spectrum in the paraxial approximation is given by

$$\mathbf{E}\left(k_{rx}, k_{ry}, z_r\right) = \mathbf{E}_0\left(k_{rx}, k_{ry}\right) e^{iz_r\sqrt{k_0^2 - k_{rx}^2 - k_{ry}^2}} \cong \mathbf{E}_0(k_{rx}, k_{ry}) e^{ik_0 z_r} e^{-\frac{i}{2k_0}\left(k_{rx}^2 + k_{ry}^2\right)z_r}, \tag{S2}$$

where $k_0 = 2\pi/\lambda$ is the incident wave vector, and k_{rx}, k_{ry} are the components of the wave-vector of the reflected beam in x_r, y_r direction.

Based on the boundary condition, the reflected angular spectrum is expressed as [2, 3]:

$$\begin{bmatrix} E_r^p \\ E_r^s \end{bmatrix} = \begin{pmatrix} r_p & \frac{k_{ry}(r_p + r_s)\cot\theta_i}{k_0} \\ -\frac{k_{ry}(r_p + r_s)\cot\theta_i}{k_0} & r_s \end{pmatrix} \begin{bmatrix} E_i^p \\ E_i^s \end{bmatrix}, \tag{S3}$$

where r_p and r_s are the Fresnel reflection coefficients for *p*- and *s*- polarizations, respectively, θ_i is the incident angle, $k_{rx} = -k_{ix}$, and $k_{ry} = k_{iy}$.

Decomposing into a Taylor series in the vicinity of the central wave vector $k_{ix0} = k_0 \sin\theta_0$, r_p and r_s can be represented as:

$$r_{p,s}(\theta_i) = r_{p,s}(\theta_0) + (\theta_i - \theta_0)\left.\frac{dr_{p,s}}{d\theta_i}\right|_{\theta_i = \theta_0} + \frac{1}{2}(\theta_i - \theta_0)^2 \left.\frac{d^2 r_{p,s}}{d\theta_i^2}\right|_{\theta_i = \theta_0} \ldots . \tag{S4}$$

Consider the incident *p*- polarized beam with a Gaussian angular spectrum:

$$E_i^p = \frac{w_0}{\sqrt{2\pi}} \exp\left[-\frac{w_0^2\left(k_{ix}^2 + k_{iy}^2\right)}{4}\right], \tag{S5}$$

where w_0 is the beam waist.

Calculating the integral in Eq. (S1) using Eqs. (S3) - (S5) and relationships $E_r^p = \frac{1}{\sqrt{2}}(E_r^+ + E_r^-)$ and $E_r^s = \frac{i}{\sqrt{2}}(E_r^- - E_r^+)$, we obtain the expression for the right- and left- handed circularly polarized components of the reflected field

$$E_r^{\pm} = \frac{1}{\sqrt{2\pi}w_0}\frac{z_R}{z_R+iz_r}\exp\left(-\frac{k_0}{2}\frac{x_r^2+y_r^2}{z_R+iz_r}\right)\left[r_{p,s} - \frac{ix_r}{z_R+iz_r}\frac{dr_{p,s}}{d\theta_i} \mp \frac{y_r\cot\theta_i}{z_R+iz_r}(r_p + r_s)\right], \quad \text{(S6)}$$

where the positive and negative signs denote the right circularly polarized (RCP) and the left circularly polarized (LCP) field components, and $z_R = k_0 w_0^2/2$ is the Rayleigh length.

In Fig. S1, the measured and calculated intensity profiles of left- handed circularly polarized components of the reflected beams passing through a CPL filter, which includes a quarter-wave plate and a linear polarizer, are presented at a distance of z = 25 cm from the *Ni* grating surface for different angles of incidence. An incident Gaussian beam with a beam waist $w_0 = 22.6$ μm is *p*- polarized. It follows from this that in-plane spin-independent beam splitting (without separation of photons with opposite spin angular momentum (SAM)), which is the Goos-Hanchen shift, occurs for an incident *p*-polarized beam. The appearance of two spots around the resonant angle of incidence is due to the presence of a dip in the reflectivity curve. It is seen from Figures S1a and S1c, that the deviation of the angle of incidence in one direction or another from the resonant angle leads to a change in the spatial position of the reflected beam.

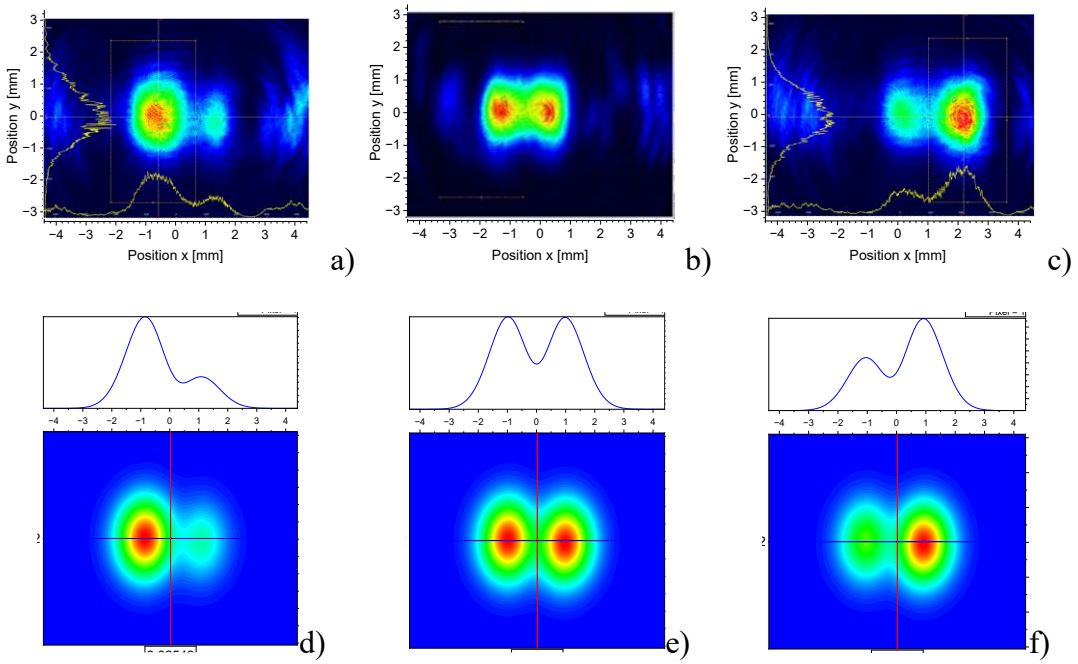

Fig. S1. Measured (a, b, c) and calculated (d, e, f) intensity profiles of reflected beams from *Ni* grating after passing through the CPL filter. (a, d) $\theta_i = 33.48°, (b, e)$ $\theta_i = 33.53°,$ (c, f) $\theta_i = 33.58°$.

To observe the enhanced in-plane spin-dependent splitting, an optimal overlap of the preselection and post-selection states should be created. This makes it possible to observe the enhancement of spin Hall shift by controlling the polarization of the incident beam, that is, by slightly changing the direction of the polarization vector of a linearly polarized incident beam relative to *p*-polarization. In this case, the incident beam becomes elliptically polarized (contains *p*- and *s*-polarization components) and the reflected beam is expressed as:

$$\begin{bmatrix} E_{rw}^{p} \\ E_{rw}^{s} \end{bmatrix} = \begin{bmatrix} r_p \cos\gamma + \frac{k_{ry}(r_p+r_s)\cot\theta_i \sin\gamma}{k_0} \\ r_s \sin\gamma - \frac{k_{ry}(r_p+r_s)\cot\theta_i \cos\gamma}{k_0} \end{bmatrix} \tilde{E}_i(k_{ix}, k_{iy}), \tag{S7}$$

where γ is the linear polarization angle of incident beam (preselection angle) between the polarization vector and axis x_i, and $\tilde{E}_i$ is the Gaussian angular spectrum.

For this preselection, the in-plane spin splitting undergoes significant amplification. It follows from Eq. (S7) that the center of gravity (centroid position) of the circularly polarized component of the reflected beam is expressed as

$$\langle x^{\pm} \rangle = \frac{\langle E^{\pm}|x|E^{\pm}\rangle}{\langle E^{\pm}|E^{\pm}\rangle} = \frac{\iint x|E^{\pm}|^2 dxdy}{\iint |E^{\pm}|^2 dxdy} = \frac{2\sqrt{z_R^2+z_r^2}\,|\dot{r}_p|\cos\gamma(a_p\cos\gamma \mp a_s\sin\gamma)}{2k_0 z_R(a\pm b)+|\dot{r}_p|^2\cos^2\gamma}, \tag{S8}$$

where $E^{\pm}$ are the electric fields that are right- and left- handed circularly polarized, respectively, $a_p = -|r_p|\sin(\varphi_p + \gamma_1 - \gamma_2)$; $a_s = |r_s|\cos(\varphi_s + \gamma_1 - \gamma_2)$; $a = |r_p|^2\cos^2\gamma + |r_s|^2\sin^2\gamma$; $b = |r_p||r_s|\sin(2\gamma)\sin(\varphi_p - \varphi_s)$, $z_R + iz_r = \sqrt{z_R^2 + z_r^2}\,e^{i\gamma_1}$, $z_R = k_0 w_0^2/2$, $r_p = |r_p|e^{i\varphi_p}, r_s = |r_s|e^{i\varphi_s}$, φ_s and φ_p are the phases of the Fresnel reflection coefficients r_p and r_s, respectively$_s$ $\dot{r}_p = |\dot{r}_p|e^{i\gamma_2}$, $\dot{r}_p = \frac{\partial r_p}{\partial \theta_i}$.

A rigorous electromagnetic theory based on the *C*- method is used for the calculations of the reflection coefficients r_p and r_s [4-6]. Optimal conditions for the coupling of incident light with a surface plasmon wave is achieved at a grating depth of h = 80 nm and a resonant angle of incidence of $\theta_{res} = 33.53^{o}$, corresponding to the optimal condition for the coupling of incident light with a surface plasmon. In this case the minimum reflection from the grating is achieved. As the grating depth differs from the optimal, the value of the minimum reflection coefficient increases. The optimal depth depends on the grating period and material [4-6]. It was shown that the optimal depth for the silver grating is h = 20 nm.

At the optimal preselection angle, we clearly observe the in-plane angular splitting of reflected light with opposite circular polarizations. The optimal preselection angle corresponds to the condition under which the amplitude of reflected light with *p*- polarization becomes equal to the amplitude of reflected light with *s*-polarization.

In Fig. S2, the in-plane spin splitting for the preselection angle $\gamma = 4°$ is shown for a nickel grating with a period of $\Lambda = 400$ nm and a depth of $h = 80$ nm at a wavelength of radiation $\lambda = 632.8$ nm with *p*- polarization. The dielectric constant of nickel at the wavelength $\lambda = 632.8$ nm is $\varepsilon = -10.1 + i14.73$. Note that an *s*- wave does not excite surface plasmon waves, so a *p*- polarized incident wave is necessary to observe the surface plasmon resonance.

When the reflected beam passes through a filter of a certain circular polarization, one of the spots disappears. This means that there is a spatial separation of left-handed and right-handed circularly polarized photons. At a preselection angle of $\gamma = 4°$, the right spot is left-handed circularly polarized, while the left spot is right-handed circularly polarized. On the contrary, at $\gamma = -4°$, the right spot is right-handed circularly polarized, and the left spot is left-handed circularly polarized. The physical mechanism of such separation is related to the spin-orbit interaction enhanced by surface plasmon resonance in a subwavelength diffraction grating.

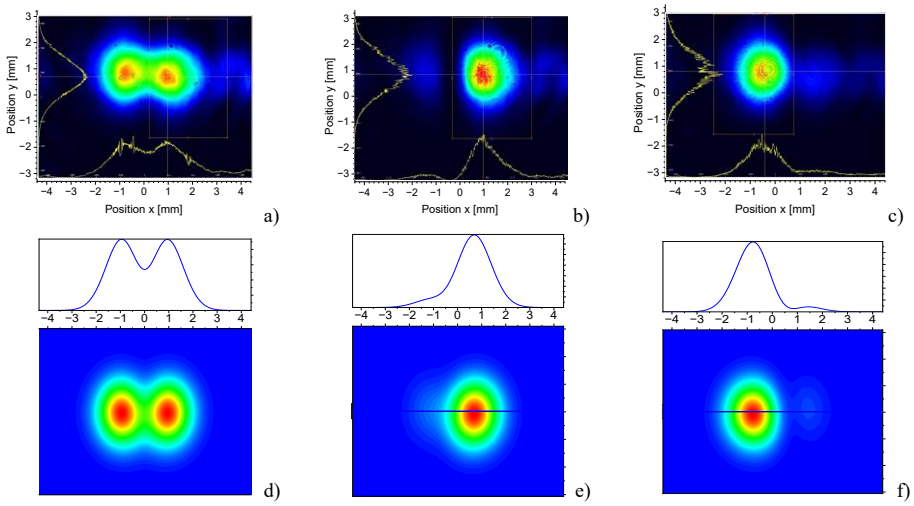

Fig. S2. Measured (a, b, c) and calculated (d, e, f) intensity profiles of the reflected beams at a distance of $z = 25$ cm from the *Ni* grating surface. $\theta_i = \theta_{res} = 33.53°$, $\gamma = 4°$. (a, d) without polarizers, (b, e) after passing the LCP filter, and (c, f) after passing the RCP filter.

In Fig. S3, the measured and calculated intensity profiles of left- handed and right-handed circularly polarized components of the reflected beams are presented at a distance of z = 22 cm from the *Ag* grating surface.

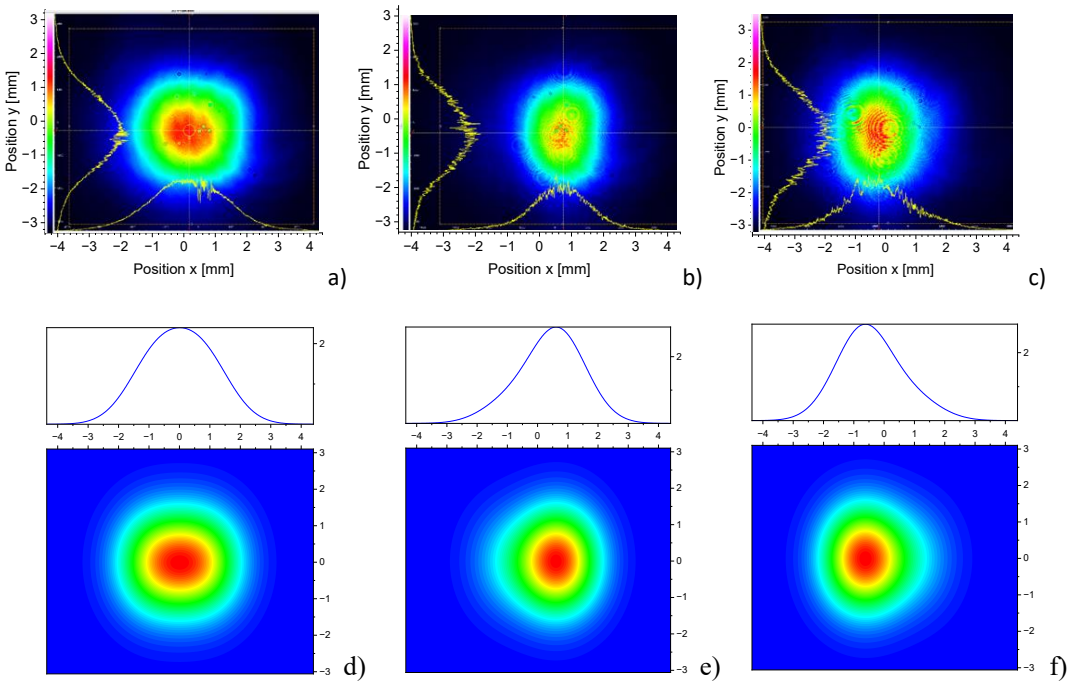

Fig. S3. Measured (a, b, c) and calculated (d, e, f) intensity profiles of the reflected beams at a distance of $z = 22$ cm from the *Ag* grating surface. $\theta_i = \theta_{res} = 33.30°$, $\gamma = 60°$. (a, d) without polarizers, (b, e) after passing the LCP filter, and (c, f) after passing the RCP filter. $\Lambda = 400$ nm, $h = 20$ nm, $\lambda = 632.8$ nm.

The LCP and RCP (left-handed and right-handed circularly polarized) components of the reflected beam are well separated along the *x* axis, i.e., they are shifted in opposite directions. The left and right spots have circular polarizations with opposite signs of helicity. Photons with a given helicity are shifted in the opposite direction when the preselection angle changes its sign. This demonstrates the possibility of switching the spatial position of reflected beams with opposite helicity signs by slightly changing the polarization angle of the incident beam.

In Fig. S4, the influence of the preselection angle on the position of the reflected beam with the left-handed circular polarization is shown. When choosing the optimal preselection angle, a high degree of spin separation is achieved.

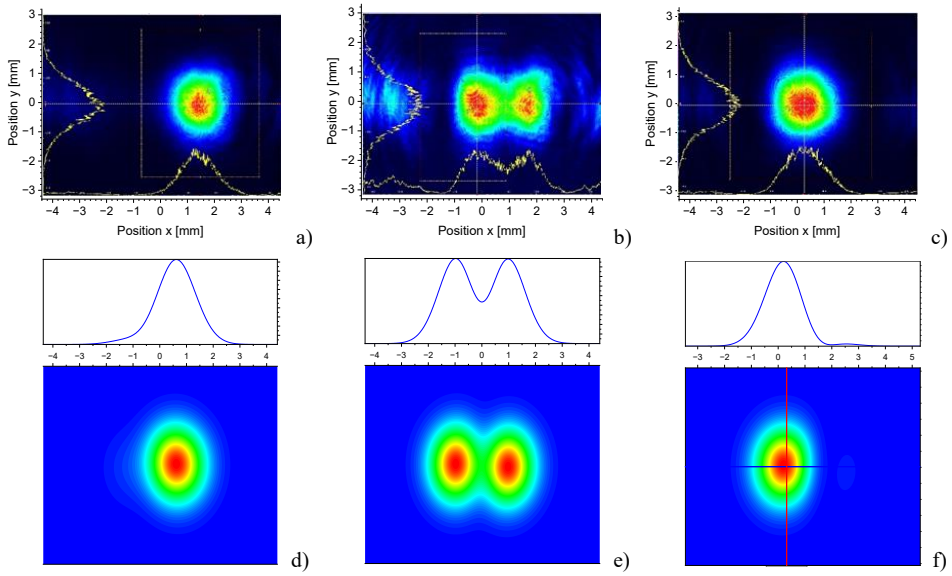

Fig. S4. Measured (a, b, c) and calculated (d, e, f) intensity profiles of reflected beams passing through the LCP filter at a distance of z = 25 cm from the *Ni* grating surface. $\theta_i = \theta_{res} = 33.53°$, (a, d) γ = -4°, (b, e) γ = 0°, and (c, f) γ = 4°.

It can be seen, that there is no photon spin Hall effect (PSHE) at the preselection angle γ = 0° (Figs. S3b and S3e). However, the apparent spin splitting occurs at a nonzero preselection angle reaching the maximum separation distance between beams with opposite circular polarization at $\gamma = \pm 4°$ (Figs. S3a and S3c). The measurements show that the positions of the centroids are in good agreement with the simulation results.

The degree of separation of circular polarization components (spin separation purity) is almost zero at the preselection angle γ = 0°. This indicates the absence of a spin-dependent shift between the left- and right- circularly polarization components. However, if a non-zero preselection angle is selected, the PSHE can be clearly observed. At the optimal polarization angle of the incident beam (preselection angle), the maximum degree of polarization (DOP) and the maximum degree of spin separation are achieved. Outside the resonance angle region, the reflected light is predominantly *p*- polarized.

Thus, spin-dependent and spin-independent angular shifts enhanced by surface plasmon resonance (SPR) have been theoretically and experimentally demonstrated. In contrast to the conventional transverse spin splitting, which is an analogue of the Imbert-Fedorov shift, here we observe longitudinal spin splitting, which is significantly superior to transverse spin splitting.

1. K. Y. Bliokh and A. Aiello, Goos-Hänchen and Imbert-Fedorov shifts: an overview, J. Opt. **15**, 014001 (2013).
2. K. Y. Bliokh and Y. P. Bliokh, Conservation of angular momentum, transverse shift, and spin Hall effect in reflection and refraction of an electromagnetic wave packet, Phys. Rev. Lett. **96**(7), 073903 (2006).
3. H. Luo, X. Zhou, W. Shu, S. Wen, and D. Fan, Enhanced and switchable spin Hall effect of light near the Brewster angle on reflection, Phys. Rev. A **84**, 043806 (2011).
4. N.I. Petrov, V.A. Danilov, V.V. Popov, B.A. Usievich, Large positive and negative Goos-Hänchen shifts near the surface plasmon resonance in subwavelength grating, Opt. Express **28**(5), 7552-7564 (2020).
5. N.I. Petrov, Y.M. Sokolov, V.V. Stoiakin, V.A. Danilov, V.V. Popov, B.A. Usievich, Observation of Giant Angular Goos-Hanchen Shifts Enhanced by Surface Plasmon Resonance in Subwavelength Grating, Photonics **10**, 180 (2023).
6. N.I. Petrov, Y.M. Sokolov, V.V. Stoiakin, V.A. Danilov, V.V. Popov, B.A. Usievich, Direct observation of the enhanced photonic spin Hall effect in a subwavelength grating, Opt. Lett. **50**, 1317-1320 (2025). DOI: 10.1364/OL.549579